International Journal of Science and Research (IJSR)
ISSN: 2319-7064
SJIF (2022): 7.942

Development of Structural and Electrical Properties of Freestanding Silicon Membrane Doped Lithium

M. Jaouadi[1, 2], H. Ezzaouia[2]

[1]Physical Sciences Department, College of Science, Jazan University, P. O. Box.114, Jazan 45142, Kingdom of Saudi Arabia
Corresponding Author. Email: *maljuwadi[at]jazanu.edu.sa, mohja05.08[at]hotmail.com*
Tel: +966553052392

[2]Laboratoire de Photovoltaïque, Centre de Recherches et des Technologies de l'Energie, Technopole de Borj - Cedria, BP 95 Hammam - Lif 2050, Tunisia

Abstract: ***Proton exchange membrane fuel cells (PEMFC) are emerging as a significant contributor to a more environmentally friendly and sustainable future as an energy conversion solution. However, the choice of cell component material offers a novel option for acquiring a high - performance fuel cell Proton exchange membrane has functions of proton transfer and electrode isolation in fuel cell. In this line, Proton conducting composite membrane was developed by impregnation of lithium bromide solution (LiBr) into mesoporous silicon, which was prepared using electrochemical etching process. The incorporation of lithium in the mesoporous structure reveal differences in surface morphology as shown by scanning electron microscopy (SEM). It's observed that the electronic conductivity of the freestanding mesoporous silicon membrane (MFr) was significantly enhanced by approximately two orders of magnitude through lithium doping. Furthermore, electrochemical impedance spectroscopy (EIS) is used to simulate the different resistances of the fuel cell membrane and effectively explains the improved performance of the composite membranes. These results demonstrate the successful integration of a new class of protonic conductor into a microfabricated silicon fuel cell.***

Keywords: Free - standing mesoporous silicon membrane (MFr), Lithium Bromide (LiBr), I (V) measurement, Electrical conductivity, Electrochemical impedance spectroscopy

1. Introduction

Hydrogen fuel cells are increasingly becoming an attractive and sustainable technology, offering numerous advantages that support a shift towards a clean energy future [1], it can provide the electrical energy consumed by automobiles, as well as some household and industrial applications with minimal environmental impacts [2]. One crucial element of these cells is the proton exchange membrane. This membrane plays an integral role in PEMFC, it has functions of proton transfer separated oxidants from fuels and electrode isolation [3]. Silicon technology remains a key enabling technology that extends towards the development of membrane technology, owing to its exceptional mechanical properties, such as high strength, stiffness, repeatability, and lack of mechanical hysteresis. Since the pioneering work of T. Pichonat *[*4], porous silicon structured has been intensively investigated as a potential candidate membrane material for fuel cell application from both economic and environmental aspects [5]. Nevertheless, a significant challenge associated of porous silicon lies in its poor rate proton conductivity, which is attributed to its high level of electronic conductivity. To overcome these obstacles, there has been a strong focus on developing membranes with exceptional physicochemical properties, two approaches have been attempted in this regard. One approach involves enhancing electronic conductivity through techniques such as pore impregnation, doping with conductive lithium ions or the use of grafted molecules [6]. Additionally, porous silicon, with its diverse range of morphologies, has been utilized for the incorporation of metals, molecules, and conducting polymers, enabling the creation of gas or biosensors. Numerous studies have been published regarding the electrical properties of porous silicon (PS) [7, 8]. However, there is a scarcity of literature pertaining to the utilization of hygroscopic hydrophobic solutions, specifically lithium bromide aqueous solutions, to fill porous silicon structures, investigate their electrical behavior, and achieve enhanced conductivity [9]. The porous structure and size can be adjusted based on the specific aim of investigations or applications. The Li/Si alloying reaction induces a large volume expansion (310 %) causing material pulverization which leads to active material electrical isolation. To address this issue, a comprehensive morphological study has been conducted [10]. In conjunction with structural characterization, I - V analysis yields a complete understanding of the different phenomena occurring in the specimen before and after the doping effect can be obtained. The major advantage of I - V measurements lies in their ability to differentiate between individual contributions to the electrical conduction of porous silicon, both before and after the doping effect. In this research investigation, we aim to explore the measurement of impedance measurement with respect to frequency allows one to inspect the detailed physical processes inside materials through their electrical analogy [11]. The most important advantage of the EIS study is its capacity to distinguish the individual contributions to electrical conduction or polarization from various sources, such as porous silicon, LiBr salts, contact regions, and electrode–sample interface where defects are generated.

2. Experimental Details

The tremendous appeal of PS lies in its capacity to modify the properties of silicon through the introduction of nano - and microscale porosity into the material. Furthermore, the development of highly efficient membranes presents a fabrication challenge. The proton exchange membrane (PEM) determines the working mode and performance of the PEMFC. A wide range of electrolytes and membranes has been proposed for operation in low - temperature PEMFC. In

the present study, freestanding PS samples were prepared from p^+ type (100) Si wafers with a resistivity of 0.01–0.001 Ω cm at room temperature. Electrochemical etching was conducted using a galvanostat in an HF: C_2H_5OH solution, with a weight ratio of 1: 1. A gradient porosity is necessary to ensure bi - porous layer. A Current density of 30 mA/cm^2 was applied for 15 minutes, followed by a second current density of 60 mA/cm^2 was applied for 15 min. The current density was subsequently increased to detach the bi - porous layer from it' s bulk. This process has no effect on the intrinsic properties of Psi but it has impact of the properties of PS - based devices. By removing the bulk silicon below a PS layer and creating a membrane, a whole new set of physical and chemical characteristics, as well as potential applications, have been discovered. Novel methods for fabricating and integrating MFr membrane have been developed, increasingly relying on semiconductor microfabrication techniques. However, after the formation of bi - porous silicon layers, the freestanding membrane is immersed in aqueous lithium bromide solution with S/3 concentration (S=1.66 g/ml) to ensure pore doping, following previously described processes [9]. A thorough analysis of the advantages and disadvantages of this material was conducted.

3. Results and Discussion

3.1 Structure of freestanding membrane - based on porous silicon doped lithium

The thickness of the bi - porous layer that was achieved was determined using cross - sectional scanning electron microscopy (SEM). Figure 1 (a) exhibits that the thickness of the mesoporous silicon measures approximately 51 µm, and the structure of the mesoporous silicon layer appears columnar. Various pore diameters can be achieved to cater to different filtration ranges.

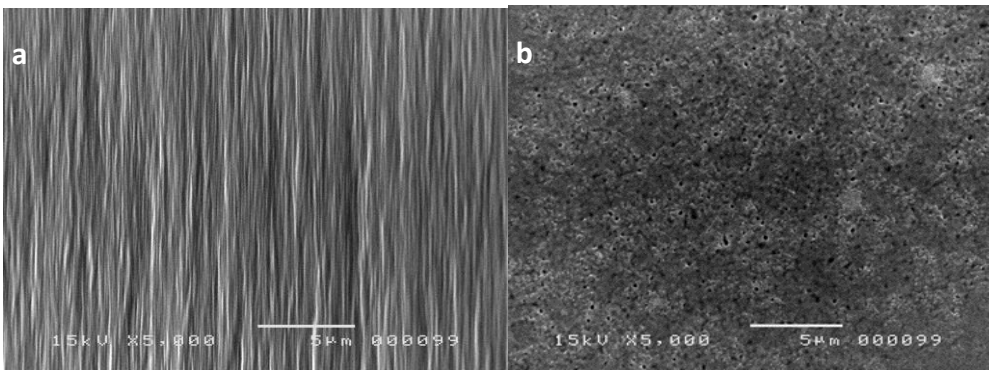

Figure 1: Mesoporous freestanding silicon membrane (a) SEM morphology of the freestanding showing the pores, and (b) cross - section SEM images of silicon membrane showing the thickness.

A significant dependence on size to fracture was discovered. Specifically, a critical particle diameter of approximately 150 nm was identified, below which the particles did not crack or fracture upon first lithiation [10]. Particles above this critical diameter experienced surface cracks initially and then fractured due to lithiation - induced swelling [10]. The porous structure and size vary based on the specific objective of the investigation. However, before lithium doping, the size of the mesoporous silicon measures approximately 146 nm, as depicted in figure 1 (b). The impregnation of LiBr into the pore has been confirmed by the SEM on the cross - section of the LiBr/PS system Figure 2, the structure has been annealed at 550 °C for 15 min under oxygen. It can be clearly seen visually the white clusters of LiBr on PS pores.

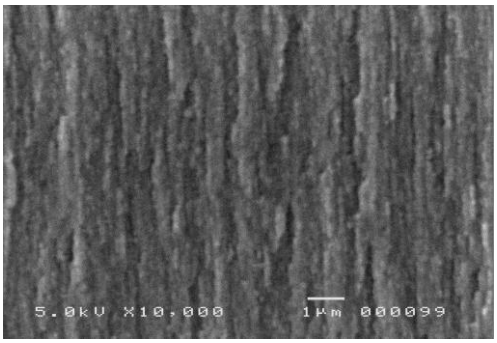

Figure 2: Confirmation of LiBr impregnation into the pore by Cross sectional SEM of the LiBr/PS system.

3.2 Electrical Properties

The electrical characterization of the heterostructure conducted by depositing silver contacts on both sides of the freestanding LiBr/PS system, figure 3 shows the top real view of the membrane. The contact area measured 80 mm^2.

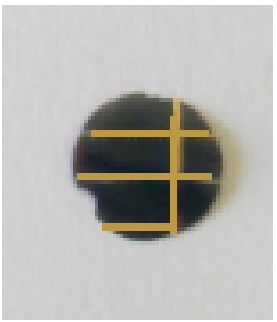

Figure 3: Real Top - view of the Fabricated freestanding membrane.

The current - voltage (V - I) characteristics were then measured. Figures 4 (a) and 4 (b) plots cell potential versus current of mesoporous silicon freestanding before and after lithiation, respectively.

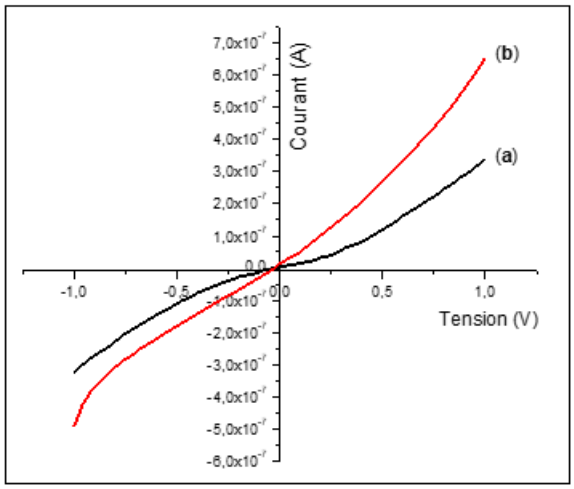

Figure 4: Comparison of the I - V characteristics before and after lithium doping of the mesoporous silicon bi - layer Au/ LiBr/ PS/ Au system

The forward current of the mesoporous silicon bi - layer structure was initially low, but increased after lithium doping. **Table 1** provides a concise summary of the membrane resistances and conductivity prior to and following lithiation. The resistance of porous layer was calculated before and after impregnation according to the following equation:

$$R^{SP} = \rho^{SP} e/S \qquad \text{(Eq.1)}$$

Where ρ^{SP}, e resistivity and thickness of porous layer respectively, and S the area of metallic layer deposited on porous layer.

Table 1: The effect of impregnation process on the values of resistances of mesoporous silicon layer

Free - standing membrane Before lithiation	After lithiation
Resistance R^{SP} = 35 10^5 Ω	R^{SP}= 20 10^5 Ω
Conductivity σ=0.014 Ω/cm	σ =0.025 Ω/cm

The electrical conductivity of MFr experiences a notable enhancement of approximately two orders of magnitude after to lithium pore - filling. The conductivity enhancement can be attributed to the passivation of lithium, which enhances the mobility of charge carriers, as well as the diffusion of metallic spaces within the porous matrix. The lithiation of MFr facilitates the process of proton conduction by reducing the resistance associated with proton conduction within the hydrophilic membrane.

3.3 Impedance characteristics

The freestanding mesoporous silicon membranes doped lithium was tested in this study, the active area of cell is 80 mm^2. The AC impedance measurements were carried out by an Autolab PG STAT 30. The impedance spectra were recorded by sweeping frequencies over the range of 1 Hz to 10 kHz. The amplitude of the AC current was always kept at 10% of the DC current. The membrane with large active area of 80 mm^2 was operated steadily for at least 5 mn before starting impedance measurement.
Figure 5 shows a typical Nyquist plot of a proton exchange membrane for fuel cells application using Z - view software. The plot depicts two distorted capacitive semicircles in the upper plane. The first capacitive loop in the higher frequency range is related to the electrochemical reaction and the second loop is closely related to the mass transfer reaction in the middle frequency range. The intersection point on the horizontal axis at higher frequency is usually attributable to the internal resistance of the membrane [12].

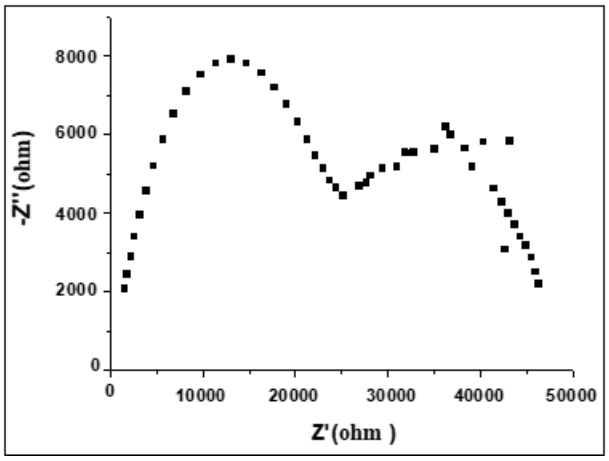

Figure 5: Nyquist plot for the mesoprous freestanding silicon membrane impregned by lithium bromide solution.

Often, a rough or porous surface can cause the capacitance to appear as a constant phase element (Q), which is used in a model in place of a capacitor to compensate for the non - ideal conditions in the system [13, 14]. Thus, an equivalent circuit was proposed to describe the mechanism under investigation, as shown in the inset of Fig.6. R_s, R_1 and R_2 represent the internal resistance (R_s), the resistance of the electrochemical reaction (charge transfer) and the resistance of the mass transfer reaction (diffusion), respectively. Q_1 and Q_2 are constant phase elements of the charge transfer reaction and the diffusion, respectively. The experimental EIS measurement is plotted with the theoretically predicted curve based on the proposed equivalent circuit shown in Fig.6.

The spectra of Fig.6 consist typically of a high frequency two overlapping arcs in high and medium frequency regions. The high frequency intercept part (intersection with the real axis in impedance spectrum) reflects the ohmic resistance of membrane (R_{ohm}); the arc at high frequency reflects the combination of charge transfer resistance (R_{ct}) due to the oxygen reduction reaction and double layer capacitance within the catalyst layer, which is considered to be a constant phase element (Q_1); the arc at medium frequency reflects the mass transport resistance of oxygen in the catalyst layer (R_{mt}) and the associated constant phase element (Q_2). Capacitance (Q) is the element commonly used in the conventional equivalent circuit model. In the case of a porous specimen with rough surface. In this work, Q is used since the specimens are porous.

The measured electrochemical impedance spectra are fitted using Z - view software. Figure 6 shows that the fit is in good agreement with the experimental result. The values of the different fitting parameters of the equivalent circuit model assigned to the mesoporous freestanding silicon membrane after pore filling in good agreement with the calculated conductivity summarized in table 1 that deduced from equation (2).

$$\frac{\sigma_1{}^{SP}}{\sigma_2{}^{SP}} \cong \frac{\rho_1{}^{SP}}{\rho_2{}^{SP}} \cong \frac{R_{before}}{R_{after}} \quad \text{(Eq.2)}$$

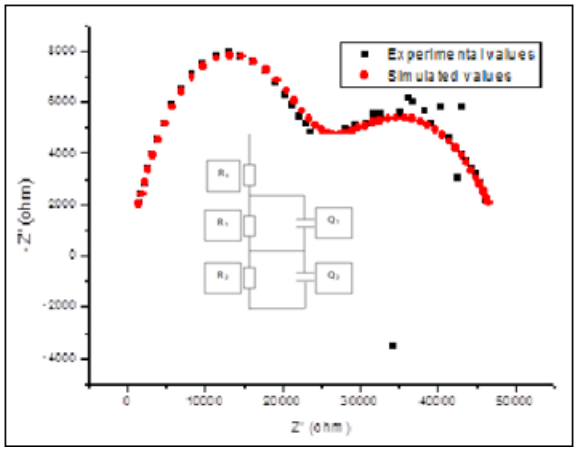

Figure 6: Nyquist plot is plotted with the curve fitted based on the proposed equivalent circuit.

4. Conclusion

In manufacturing of proton exchange membrane for fuel cell application, we have used silicon nanocrystals as the supporting framework impregnate with lithium bromide to enhance conductivity. This structure improved the overall performance of the prepared fuel cells membrane as a result of the high surface area and gradient porosity of mesoporous free - standing silicon membrane. The thickness of membrane, size of pore, and lithium incorporation was confirmed by examining SEM morphology.

By studying the Au/LiBr/PS/Au structure, we discovered that the ohmic resistance derived from an I - V diagrams is equal to half of the ohmic resistance before doping for Au/PS/Au structure. This paper introduced an EIS diagnostic method that provide some useful information we have identified two arcs, the impedance model resulting in excellent matches between the simulation results and the experimental data in the Nyquist. By simulating the equivalent circuit, we conclude that the ohmic resistance calculated in good agreement with the fitted one, an enhancement performance of the composite membranes was shown for doped structure. The fuel cell membrane prepared can be adapted for the production of highly efficient and robust composite thin films for efficient energy conversion.

References

[1] Z. Xu, D. Qiu, P. Yi, L. Peng, and X. Lai, Prog. Nat. Sci. Mater. Int.30**, 815**, (2020).
[2] Jiao, K., Xuan, J., Du, Q., et al. Nature **595**, (2021), 361–369.
[3] So - Yeon Choa, Ki - Won Lee, Jae - Wan Kim, Dong - Hyun Kim, Sensors and Actuators B: Chemical **183**, (2013), 428–433.
[4] T. Pichonat, B. Gauthier - Manuel, D. Hauden, Chem. Eng. J.1**01** (1–3) (2004) 107–111.
[5] M. Jaouadi, W. Dimassi, M. Gaidi, R. Chtourou, H. Ezzaouia, Applied surface science, **258** (2012) 5654 – 5658.
[6] Cano, Z. P., Banham, D., Ye, S. Y., et al.: Batteries and fuel cells for emerging electric vehicle markets. Nat. Energy **3**, (2018), 279–289.
[7] A. S. Mogoda, Y. H. Ahmad, W. A. Badawy, Materials Chemistrey and Physics, **126, (**2011) 676 - 684.
[8] Jonathan E. Spanier, Alan C. West and Irving P. Herman, Journal of The Electrochemical Society, **148** (10), (2001), C663 - C667.
[9] M. Jaouadi, M. Gaidi and H. Ezzaouia, Superlattices and Microstructures **54**, (2013), 172–180.
[10] X. H. Liu, L. Zhong, S. Huang, S. X. Mao, T. Zhu, J. Y., ACS Nano.6, (2012), 1522–1531.
[11] Hung - Chung Chien, Li - Duan Tsai, Chien - Ming Lai, Jiunn - Nan Lin, Chao - Yuan Zhu, Feng - Chih Chang, Journal of Power Sources **226, (**2013), 78 - 93.
[12] XiqiangYan, Ming Houb, Liyan Sun, Dong Liang, Qiang Shen, Hongfei Xu, Pingwen Ming, BaolianYi, International Journal of Hydrogen Energy **32, (**2007), 4358 – 4364.
[13] T. L. Kulova, A. M. Skundin, Yu. V. Pleskov, O. I. Kon'kov, E. I. Terukov and I. N. Trapeznikova, Chem. Biochem. Eng. Q., **21** (4), (2007), 83–92.
[14] Ning - Yih Hsu, Shi - Chern Yen, King - Tsai Jeng, Chun - Ching Chien, J. Power Sources**, 161, (**2006), 232–239